

published), and Ref. 14. The last two also discuss the  $3^*$  model. V. Barger, D. V. Nanopoulos, and R. J. N. Phillips, University of Wisconsin Report No. COO-881-

537 (to be published); S. Pakvasa, H. Sugawara, and M. Suzuki, Lawrence Berkeley Laboratory Report No. LBL 6419 (to be published).

## Spin Analysis of Charmed Mesons Produced in $e^+e^-$ Annihilation

H. K. Nguyen,<sup>(a)</sup> J. E. Wiss, G. S. Abrams, M. S. Alam, A. M. Boyarski, M. Breidenbach, R. G. DeVoe, J. Dorfan, G. J. Feldman, G. Goldhaber, G. Hanson, J. A. Jaros, A. D. Johnson, J. A. Kadyk, R. R. Larsen, D. Lüke, V. Lüth, H. L. Lynch,<sup>(b)</sup> R. J. Madaras, J. M. Paterson, M. L. Perl, I. Peruzzi,<sup>(c)</sup> M. Piccolo,<sup>(c)</sup> F. M. Pierre,<sup>(d)</sup> T. P. Pun, P. Rapidis, B. Richter, R. F. Schwitters, W. Tanenbaum, and G. H. Trilling

Lawrence Berkeley Laboratory and Department of Physics, University of California, Berkeley, California 94720, and Stanford Linear Accelerator Center, Stanford University, Stanford, California 94305

(Received 6 June 1977)

We have studied the threshold production and decay angular distribution of neutral charmed mesons produced in  $e^+e^-$  annihilation. We find consistency with the expected spin values of 0 and 1 for the ground and excited states  $D$  and  $D^*$ , respectively. We rule out the alternative spin assignment of 1 for the  $D$  and 0 for the  $D^*$ .

We report on a study of the production and decay angular distributions of neutral charmed mesons<sup>1</sup> produced in  $e^+e^-$  annihilation at center-of-mass energies near 4.03 GeV. Throughout this Letter, we identify the neutral state decaying into  $K\pi$  and  $K3\pi$  at 1865 MeV/ $c^2$  with the  $D^0$  and the charged state decaying into  $K\pi\pi$  at 1875 MeV/ $c^2$  with the  $D^+$ .<sup>2</sup> A study<sup>3</sup> of the threshold recoil spectrum against the  $D^0$  and  $D^+$  has provided strong evidence for the existence of excited charmed states: the  $D^{*0}(2005)$  and the  $D^{*+}(2010)$ . Furthermore, this study shows that  $D^0$  production near threshold is dominated by two-body reactions such as

$$e^+e^- \rightarrow D^0\bar{D}^{*0} \text{ or } \bar{D}^0D^{*0}, \quad (1)$$

$$e^+e^- \rightarrow D^{*0}\bar{D}^{*0}, \quad (2)$$

$$e^+e^- \rightarrow D^{*+}D^- \text{ or } D^{*-}D^+, \quad (3)$$

where the  $D^{*0}$  and  $D^{*+}$  decay into  $D^0$ 's via pion emission<sup>4</sup> and, in the case of the  $D^{*0}$ , by  $\gamma$  emission. In this Letter we examine angular distributions in Reactions (1) and (2) in order to test the three possible  $D$ ,  $D^*$  spin assignments if one assumes that the sum of the spins for the  $D$  and the  $D^*$  is less than 2. We show that under this assumption the  $D$  is spinless, the  $D^*$  has spin 1, and their relative parity is even.<sup>5</sup>

Considerable information on the spin and parity of the  $D$  and  $D^*$  comes from a study of the  $D^*$  production and decay modes. Our observation of

either  $D^{*0} \rightarrow D^0\gamma$  or  $D^{*0} \rightarrow \pi^0D^0$  produced in  $e^+e^- \rightarrow D^0\bar{D}^{*0}$  or  $\bar{D}^0D^{*0}$  implies that the  $D$  and  $D^*$  cannot both be spinless.<sup>6</sup> Observation of  $D^* \rightarrow D\pi$  implies that  $D$  and  $D^*$  must have even relative parity if one meson has spin 0 and the other has spin 1. This last observation is quite helpful for it allows unique predictions for the production and decay angular distributions of  $D \rightarrow K\pi$  in Reaction (1) under the two spin assignments which we will further consider:  $J_D = 0$  and  $J_{D^*} = 1$ , or  $J_D = 1$  and  $J_{D^*} = 0$ .

We express the expected joint  $D^0$  production and decay distributions in terms of the three angles  $\Theta$ ,  $\theta$ , and  $\varphi$ , where  $\Theta$  is the polar production angle of the  $D^0$  with respect to the annihilation axis, and  $\theta$  and  $\varphi$  are the spherical angles of the decay kaon in the  $D^0$  helicity frame.<sup>7</sup> In the limit of nonrelativistic  $D^{*0}$ 's, one computes from symmetry considerations the distributions below<sup>8</sup>:

$$\frac{d^3\sigma}{d\cos\Theta d\cos\theta d\varphi} \propto 1 + \cos^2\Theta, \quad (4)$$

$$\frac{d^3\sigma}{d\cos\Theta d\cos\theta d\varphi} \propto \sin^2\theta(\cos^2\varphi + \cos^2\Theta \sin^2\varphi), \quad (5)$$

where Eq. (4) is for  $J_D^P = 0^\mp$ ,  $J_{D^*}^P = 1^\mp$ , and Eq. (5) is for  $J_D^P = 1^\mp$ ,  $J_{D^*}^P = 0^\mp$ . We shall compare these distributions to the data.

The present analysis is based on about 35 000 hadron events produced in  $e^+e^-$  annihilation at

center-of-mass energies between 3.9 and 4.15 GeV. The data were taken with the Stanford Linear Accelerator Center-Lawrence Berkeley Laboratory magnetic detector at SPEAR. Descriptions of the detector and event selection procedures using time-of-flight information have been published.<sup>1,9</sup> All neutral two-prong combinations are considered as potential  $D^0$  candidates with the track having time-of-flight information most consistent with the kaon hypothesis called the kaon.<sup>10</sup> The other track is called the pion. For approximately 40% of the real  $D^0$  events this amounts to little more than a random selection. For the production angular distribution this  $K-\pi$  ambiguity is irrelevant; however, it could matter in analyzing the decay distribution of the kaon in the  $D^0$  helicity frame. Fortunately we find that it does not, since  $K-\pi$  interchange effectively reverses the direction of the kaon in the  $D^0$  helicity frame, and the angular distributions we are testing are invariant under this transformation.

A relatively clean sample of  $D^0$ 's produced against  $\bar{D}^{*0}$ 's in Reaction (1) can be selected by cutting on the invariant mass of the  $K\pi$  system and the corresponding recoil mass. We have obtained a sample of 153  $D^0$  candidates by cutting on invariant mass from 1820 to 1920  $\text{MeV}/c^2$  and on recoil mass, computed with a fixed  $D^0$  mass of 1865  $\text{MeV}/c^2$ , from 1970 to 2030  $\text{MeV}/c^2$ . About 70% of these  $D^0$  candidates were obtained at the fixed center-of-mass energy of 4.028 GeV. We estimate that approximately 15% of the  $D^0$  candidates satisfying these cuts are not  $D^0$ 's but are background two-prong combinations. Furthermore, we estimate that  $(64 \pm 4)\%$  of the real  $D^0$ 's within this cut are primary  $D^0$ 's recoiling against  $\bar{D}^{*0}$ 's. The remaining  $D^0$ 's come from either pion or  $\gamma$  decays of the  $D^{*0}$ 's produced via Reaction (1), or pion decays of the  $D^{*+}$  produced in Reaction (3).

Figures 1(a) and 1(b) show the observed  $\cos\Theta$  and  $\cos\theta$  distributions for  $D^0$  candidates satisfying the above mass and recoil-mass cuts. The normalized distributions expected for our two spin assignments are also shown. In both figures the solid curve is computed from Eq. (4) and the dashed curve is computed from Eq. (5). Both curves are calculated by a Monte Carlo program incorporating the acceptance and resolution appropriate to the SPEAR magnetic detector. The theoretical distributions have been corrected for the presence of the 15% background<sup>11</sup> and the presence of secondary  $D^0$ 's.<sup>12</sup> The difference between the solid and dashed curves of Fig. 1(a) is entire-

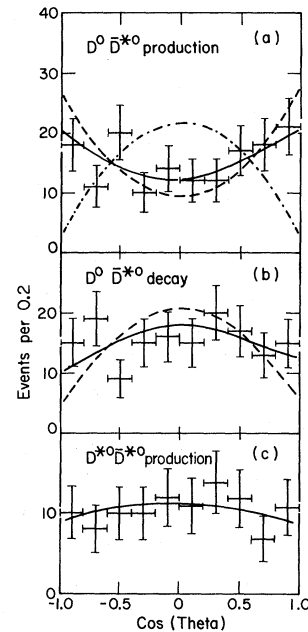


FIG. 1. (a) Production polar distribution of  $D^0$  in Reaction (1). Solid curve corresponds to  $J_D^P = 0^\pm$  and  $J_{D^*}^P = 1^\pm$ . Dashed curve corresponds to  $J_D = 1^\pm$  and  $J_{D^*}^P = 0^\pm$ . Dash-dotted curve corresponds to spinless  $D$  and  $D^*$ ; here the argument "theta" is  $\Theta$  (see text). (b) Helicity polar distribution for  $D^0$  in Reaction (1). Solid curve corresponds to  $J_D^P = 0^\pm$  and  $J_{D^*}^P = 1^\pm$ . Dashed curve corresponds to  $J_D^P = 1^\pm$  and  $J_{D^*}^P = 0^\pm$ ; here the argument "theta" is  $\theta$ . (c) Production polar distribution for  $D^0$  in Reaction (2). Solid curve is deduced from fit; here the argument "theta" is  $\Theta$ .

ly due to the effects of geometrical acceptance for the different  $D \rightarrow K\pi$  decay distributions of Eqs. (4) and (5).

Both the solid and dashed curves are acceptable fits to the data of Fig. 1(a) with the solid curve having a  $\chi^2$  of 5.6 for 9 degrees of freedom [76% confidence level (C.L.)], and the dashed curve having a  $\chi^2$  of 11 for 9 degrees of freedom (28% C.L.). The dashed and dotted curve of Fig. 1(a) is the  $\sin^2\Theta$  distribution appropriate for the case of spinless  $D$ 's and  $D^*$ 's, corrected for acceptance, background, and the presence of secondaries. This spin assignment is clearly ruled out by the data of Fig. 1(a) with a  $\chi^2$  of 74 for 9 degrees of freedom. The main discrimination between Eqs. (4) and (5) comes from the kaon polar helicity distribution shown in Fig. 1(b). The solid curve of Fig. 1(b) is consistent with the data with a  $\chi^2$  of 8.2 for 9 degrees of freedom (51% C.L.) while the dashed curve is inconsistent with a  $\chi^2$  of 23 for 9 degrees of freedom ( $6 \times 10^{-3}$  C.L.).<sup>13</sup> On the basis of this analysis the expected spin as-

segment of 0 and 1 for  $D$  and  $D^*$ , respectively, is preferred over the alternative assignment of 1 and 0.

We have devised an alternative method for comparing the data to the distribution of Eqs. (4) and (5) which makes use of all three angular variables and handles backgrounds differently. The technique displays the invariant-mass plot for events satisfying the recoil-mass cut and having variables within one of two angular regions chosen to insure discrimination between Eqs. (4) and (5) by dividing the space of angular variables by a surface of constant  $I = \sin^2\theta(\cos^2\varphi + \cos^2\Theta \sin^2\varphi)$ . Figures 2(a) and 2(b) show the  $K^+\pi^+$  invariant-mass distribution for events satisfying  $I < 0.32$  and  $I > 0.32$ , respectively. The fit of Figs. 2(a) and 2(b), consisting of a Gaussian signal over an exponentially falling background, gives  $58 \pm 8$  and  $73 \pm 10$  signal events, respectively.<sup>14</sup> Defining an asymmetry variable  $A_s$ , equal to the difference in the number of signal events over their sum, we obtain  $A_s = 0.11 \pm 0.10$  which is in good agreement with  $0.11 \pm 0.01$ , the value expected for spin-0  $D$ 's and spin-1  $D^*$ 's, but inconsistent with  $0.41 \pm 0.03$ , the value obtained for spin-1  $D$ 's and spin-0  $D^*$ 's ( $\chi^2 = 8.3$  for 1 degree of freedom;  $3.5 \times 10^{-3}$  C.L.).

In Fig. 1(c) we present the production polar distribution for  $D^0$ 's from the reaction  $e^+e^- \rightarrow D^{*0}\bar{D}^{*0}$  chosen by selecting an appropriate range in  $D^0$  momentum. About 75% of  $D^0$ 's selected come

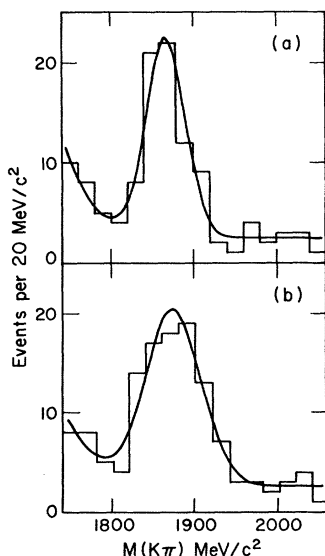


FIG. 2. Invariant-mass spectra of  $K^+\pi^+$  system for (a)  $I < 0.32$ , and (b)  $I > 0.32$ .

from the fixed center-of-mass energy of 4.028 GeV. We estimate 15% of the  $D^0$  candidates satisfying this selection are background with 75% of the real  $D^0$ 's arising from  $D^{*0} \rightarrow D^0\pi^0$  and 25% arising radiative  $D^{*0}$  decays. A  $D^0$  background sample taken from sidebands in the  $\pi K$  invariant-mass plot is consistent with isotropy.

The  $D^*$  polar distribution for the reaction  $e^+e^- \rightarrow D^*\bar{D}^*$  is of the form

$$d\sigma/d\cos\theta \propto 1 + \alpha \cos^2\theta, \quad (6)$$

where unique predictions for  $\alpha$  cannot be made by symmetry arguments except for spin 0 for which  $\alpha = -1$ .

The production polar distribution of  $D^0$  from  $D^{*0} \rightarrow D^0\pi^0$  closely follows Eq. (6) because of the low  $D^{*0}$ ,  $D^0$  relative momentum, whereas that of  $D^0$ 's arising from radiative  $D^{*0}$  decays is a broad convolution over Eq. (6) because of the larger  $D$ ,  $D^*$  relative momentum. We estimate that  $\alpha = -0.30 \pm 0.33$  by fitting the data of Fig. 1(c) to a linear combination of Eq. (6) for pionic decays, the convoluted form of Eq. (6) for radiative decays, and an isotropic background. The curve superimposed on Fig. 1(c) represents the above fit. This result is 2.1 standard deviations from the value expected for spinless  $D^*$ 's.

In summary, we have shown that the production and decay angular distributions for  $D^0$ 's produced near threshold via the reaction  $e^+e^- \rightarrow D^0\bar{D}^{*0}$  or  $\bar{D}^0D^{*0}$  are incompatible with  $D^0$ ,  $D^*$  spin and parity assignments of  $1^\mp$ ,  $0^\mp$  but compatible with  $0^\mp$ ,  $1^\mp$ . In addition the angular distribution of  $D^{*0}$ 's produced in reaction  $e^+e^- \rightarrow D^{*0}\bar{D}^{*0}$  is incompatible with spinless  $D^*$  on the 2-standard-deviation level. In the conventional quark model, one constructs the light neutral charmed mesons from an S-wave combination of a  $c$  and  $\bar{u}$  quark. In light of experience with the conventional, uncharmed mesons, one expects the  $^1S_0$  pseudoscalar charmed state to lie lower in mass than the  $^3S_1$  vector state. In this model the  $D^0$  is a pseudoscalar and the  $D^{*0}$  is a vector.<sup>15</sup> Our data are consistent with this assignment. Several theorists, however, have contemplated the alternative possibility that the  $D^0$  is a vector and the  $D^{*0}$  is a pseudoscalar.<sup>16</sup> This possibility has now been ruled out.

We wish to thank J. D. Jackson and F. Gilman for useful discussions. One of us (D.L.) wishes to acknowledge a fellowship from the Deutsche Forschungsgemeinschaft. This work was supported by the U. S. Energy Research and Development

## Administration.

<sup>(a)</sup>Permanent address: Laboratoire de Physique Nucléaire et Hautes Energies, Université Paris VI, Paris, France.

<sup>(b)</sup>Present address: DESY, Hamburg, West Germany.

<sup>(c)</sup>Permanent address: Laboratori Nazionali, Frascati, Rome, Italy.

<sup>(d)</sup>Permanent address: Centre d'Etudes Nucléaires de Saclay, Saclay, France.

<sup>1</sup>G. Goldhaber *et al.*, Phys. Rev. Lett. **37**, 255 (1976).

<sup>2</sup>I. Peruzzi *et al.*, Phys. Rev. Lett. **37**, 569 (1976).

<sup>3</sup>G. Goldhaber, Bull. Am. Phys. Soc. **22**, 20(T) (1977); G. Goldhaber *et al.*, to be published.

<sup>4</sup>G. J. Feldman *et al.*, Phys. Rev. Lett. **38**, 1313 (1977).

<sup>5</sup>Because charmed mesons are associatively produced by the strong or electromagnetic interaction, and are known to decay weakly [see J. E. Wiss *et al.*, Phys. Rev. Lett. **37**, 1531 (1976)] with parity nonconservation the absolute parity of the  $D^0$  cannot be determined and thus can be set to  $-1$  by convention.

<sup>6</sup>The presence of the decay  $D^* \rightarrow D\pi$  implies that the  $D$  and  $D^*$  have odd relative parity if both are spinless, but then they could not couple to a photon in a  $P$  wave without violating parity conservation in electromagnetic production reaction  $e^+e^- \rightarrow D^0\bar{D}^{*0}$  or  $\bar{D}^0D^{*0}$ . This seems to be one of the dominant production modes for charmed mesons near threshold (see Ref. 3).

<sup>7</sup>The helicity frame is oriented with its  $z$  axis (polar axis) along the direction of the  $D$  momentum in the over-

all center of mass and its  $y$  axis along the production-plane normal.

<sup>8</sup>J. D. Jackson, Lawrence Berkeley Laboratory Internal Note JDJ/76-1 (unpublished).

<sup>9</sup>J.-E. Augustin *et al.*, Phys. Rev. Lett. **34**, 233 (1975).

<sup>10</sup>Neutral two-body combinations with both tracks lacking time of flight are dropped from the analysis. This occurs for about 10% of the combinations.

<sup>11</sup>Background effects were included by the addition of a 15% isotropic background in both production and decay angular distributions. The assumption of background isotropy was checked by background events from 50 MeV/ $c^2$  sidebands in the  $K\pi$  invariant-mass distribution.

<sup>12</sup>The presence of secondary  $D^{0*}$ s only slightly distorts the  $\cos\Theta$  distribution of Fig. 1(a) because of the small momentum of the  $D^{0*}$ s in the  $D^{*0}$  rest frame for  $D^*$  pion decays.

<sup>13</sup>Errors in the calculation of the expected curves are not included in these  $\chi^2$  calculations.

<sup>14</sup>We note that there is a 1.5-standard-deviation inconsistency in the widths of the peaks of Fig. 2.

<sup>15</sup>S. L. Glashow, I. Iliopoulos, and L. Maiani, Phys. Rev. D **2**, 1285 (1970); A. De Rújula, H. Georgi, and S. L. Glashow, Phys. Rev. D **12**, 147 (1975); M. K. Gaillard, B. W. Lee, and J. L. Rosner, Rev. Mod. Phys. **47**, 277 (1975).

<sup>16</sup>G. Altarelli, N. Cabibbo, and L. Maiani, Phys. Rev. Lett. **35**, 635 (1975); S. R. Borchardt and V. S. Mathur, Phys. Rev. Lett. **36**, 1287 (1976).

## Nucleus-Nucleus Potential Deduced from Experimental Fusion Cross Sections

R. Bass

*Institut für Kernphysik der Universität Frankfurt am Main, 6 Frankfurt, Germany*

(Received 16 May 1977)

A classical analysis of recent fusion cross sections is presented. The results are consistent with a schematic model previously published by the author, and allow one to extract an empirical nucleus-nucleus potential.

It has been shown that nucleus-nucleus fusion cross sections can be predicted with remarkable accuracy from simple, classical, two-body models.<sup>1,2</sup> The basic ingredients of such models are (a) the assumption of a frozen shape of the colliding nuclei during their approach, (b) the assumption of a conservative two-body potential, and (c) the assumption of frictional forces which allow the system to be trapped in a region of attractive interaction.

The validity of this general approach appears to be well established by its success; however, disturbing ambiguities remain with respect to points (b) and (c) above. These can be resolved

only by further careful and systematic comparisons with experimental data. In order to make such a comparison meaningful, fusion excitation functions must be measured with good absolute precision ( $\leq 10\%$ ) over a large range of bombarding energies. Results which meet these requirements have been reported recently for a number of comparatively light nucleus-nucleus systems.<sup>3-8</sup> In the present Letter I examine to what extent these results are consistent with a schematic fusion model<sup>1</sup> and try to deduce an empirical nucleus-nucleus potential.

Following Ref. 1, I define a critical distance  $R_{cr} \approx R_{12}$  which marks the onset of strong friction-